Research paper

An early warning method for a slope based on the increment ratio of anchor cable internal force

Jincai Feng[1], Jiaxin Chen[2], Jian Li[3], Yu Zhang[4], Jianhua Guo[5], Hongyong Qiu[6]

Abstract: Prestressed anchor cables are active reinforcement to improve slope stability. However, the anchoring is not a permanent guarantee of stability, and the slope retains a potential risk of instability. From the perspective of the internal force of anchor cables, a new early warning method for the safety of the slope is provided, and a slope analysis model is established. With the increase in the strength reduction factor, the internal force increment curves of anchor cables under different prestresses are obtained. The point corresponding to strength reduction factors λ_1 and λ_2 represents a warning point. Key conclusions are drawn as follows: (1) The internal force of an anchor cable can be used to judge the stability of the slope strengthened by a prestressed anchor cable. (2) A warning index based on the internal force increment ratio of anchor cables is established. (3) The internal force increment ratio of anchor cables eliminates the influence of the initial prestress and is convenient for engineering applications.

Keywords: prestressed anchor cable, slope warning, the internal force increment ratio of anchor cables, safety factor

[1]Prof., School of Environmental Science and Engineering, Changzhou University, Changzhou 213164, Jiangsu Province, China, e-mail: hjxfjc@cczu.edu.cn, ORCID: 0000-0003-2482-3995
[2]MSc, School of Environmental Science and Engineering, Changzhou University, Changzhou 213164, Jiangsu Province, China, e-mail: chenjiaxinhi@qq.com, ORCID: 0000-0002-0275-061X
[3]Prof, School of Civil Engineering, State Key Laboratory of Geomechanics and Geotechnical Engineering, Institute of Rock and Soil Mechanics, Chinese Academy of Sciences, Wuhan 430071, Hubei Province, China, e-mail: lij@whrsm.ac.cn, ORCID: 0000-0003-4466-7379
[4]Prof, Water Development Group, Sichuan Water Development Group CO., LTD., Chengdu 610023, Sichuan Province, China, e-mail: 1791831879@qq.com, ORCID: 0000-0002-7650-5983
[5]Prof, School of Civil Engineering, State Key Laboratory of Geomechanics and Geotechnical Engineering, Institute of Rock and Soil Mechanics, Chinese Academy of Sciences, Wuhan 430071, Hubei Province, China, e-mail: guojianhua17@mails.ucas.edu.cn, ORCID: 0000-0003-3557-0698
[6]MSc, School of Civil Engineering, Changzhou University, Changzhou 213164, Jiangsu Province, China, e-mail: 814969307@qq.com, ORCID: 0000-0003-4354-7121

1. Introduction

As an active reinforcement technique, prestressed anchor cables are essential in improving slope stability [1–5]. For the slope reinforced with anchor cables, the stress state in the rock and soil is improved, the slope deformation is limited, and the safety factor is improved [6]. The anchoring of a highway slope is not a permanent guarantee of safety and stability. As the external load of the rock and soil mass and the internal structure change, the slope retains some risk of instability and failure [7–11]. Early warning research on slopes is significant for disaster prevention and mitigation [12–16].

Slope warning refers to determining the critical threshold of the slope in different states by exploring the corresponding changes in the mechanical parameters of the characteristic points on the slope and the state parameters of the slope and determining the different levels of early warning criteria according to the degree of instability and damage [16–20]. Scholars interested in such engineering operations have investigated slope early warning methods. They have constructed early warning models with different functions, which have provided a lot of evidence for the prevention and control of slope disasters [21–29]. Zhang [24] established a slope safety monitoring system by establishing the correlation between the highway slope deformation and the safety factor and data from on-site displacement monitoring. Li [25] used statistics pertaining to typical landslides and employed the deformation rate as the slope early warning criterion. Wu [26] proposed three-level landslide prediction and early warning criteria, including spatial landslide prediction and identification criteria, landslide state early warning criteria, and landslide time prediction criteria. Wang [27] used the curves of the relationship between the slope displacement and the strength reduction coefficient as the basis upon which to realize the real-time simulation analysis and prediction of the slope safety state suitable for the construction process. Wang [28] verified the feasibility of the landslide early warning model using the standard velocity method based on the characteristics of the slope displacement monitoring curve. Yang [29] used the force characteristics of the supporting structure to characterize the stability of a slope after reinforcement, and employed prestressed anchor cables to produce the difference between the stress increment and the allowable stress increment caused by deformation under various working conditions; the ratio of this difference to the allowable stress increment represents the stability of the slope. In summary, several studies on the slope early warning criterion are mostly conducted from the perspective of deformation. By taking the displacement parameter or displacement change rate in the limit equilibrium state of the slope as the threshold, the early warning model can be established by connecting the slope state and environmental factors.

Given the sudden increase of the internal force of the anchor cable, in addition to the early warning from the perspective of displacement, if the internal force of the prestressed anchor cable is also used as the monitoring and early warning indicator, the multi-index and multi-level method render the slope early warning results more accurate, which will further enrich the early warning work and more conducive to the evaluation of slope stability. The present work establishes a calculation model for a slope reinforced by prestressed

anchor cables. The safety factor is determined by the curves of the relationship between the displacement of the slope toe and the strength reduction coefficient. According to the relationship between the increment of the internal force of the anchor cable and the strength reduction coefficient, the early warning criterion of the slope based on the increment ratio of the anchor cable internal force is explored.

2. Stability calculation based on strength reduction

2.1. Calculation model

The schematic diagram of a prestressed anchor reinforcement slope is shown in Fig. 1. The slope gradient is $80°$, the height is 44.5 m, the elastic modulus is 25.0 GPa, the cohesion is 1 MPa, the friction angle is $40°$, and the Poisson's ratio is 0.23.
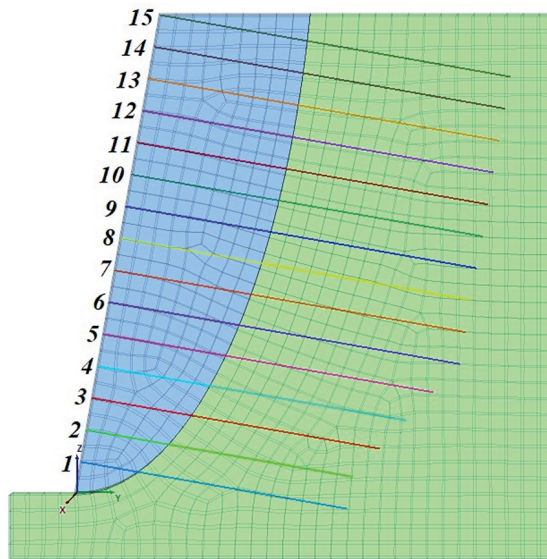

Fig. 1. Schematic diagram of the prestressed anchor cable slope

The FLAC3D strength reduction method was used to calculate the potential sliding surface of the slope instability in advance [30–40]. The slope is reinforced by 300, 350, 400, 450, 500, 550, 600, 650, 700, 750, and 800 kN anchor cables with different initial prestress; these are used to study a new early warning method based on the change of anchor cable internal force. Each anchor cable is 10 m long; from the slope toe to the top, the anchor cables are numbered 1 to 15. The model of the prestressed anchor slope is illustrated in Fig. 2.
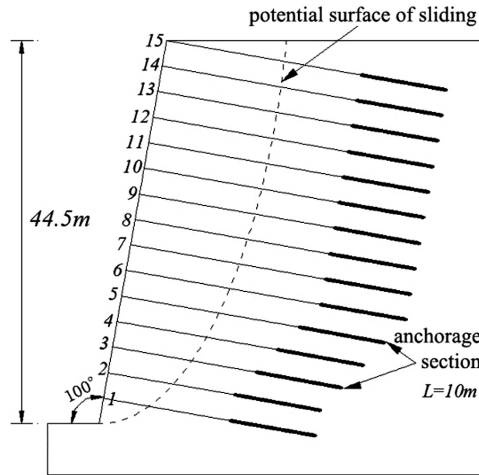
Fig. 2. Calculation model of a prestressed anchor cable slope

2.2. Safety coefficient discrimination

The stability of the slope is quantitatively investigated by the safety factor [20, 21, 26–28]. Zhao [9] took the abrupt change of node strain or displacement on the sliding surface as the sign of slope instability. In the numerical method, the safety factor can be determined by the inflection point in the curves of the relationship between the GA displacement of the slope toe and the strength reduction coefficient.
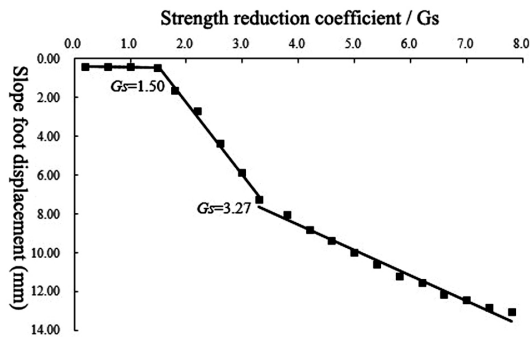

Fig. 3. The relationship between the displacement of the slope and the strength reduction factor when the prestress is 500 kN

Figure 3 shows the relationship curve between the slope toe displacement u and strength reduction factor G_s when the initial prestress is 500 kN. The curve is stable when the strength reduction coefficient $G_s < 1.50$. As the strength reduction coefficient G_s increases, the displacement of the slope toe changes little, and the slope is stable. The curve turns, and the displacement of the slope toe increases suddenly when the strength reduction coefficient

is 1.50. At this time, the slope begins to change from a stable state to an unstable state, and the slope begins to slide. When the strength reduction factor is greater than 1.5 and less than 3.27, the displacement of the slope toe increases continuously, and the slope keeps sliding. When the strength reduction coefficient is 3.27, the curve turns again, and the corresponding state is the penetration of the slope sliding surface. According to the inflection point method [12], the safety factor of the slope is 1.50.

Figure 4 shows the internal force increment diagram of anchor cables under different strength reduction factors when the initial prestress on the anchor cable is 500 kN. When the strength reduction coefficient is less than 1.50, with the increase of the strength reduction coefficient, the internal force increment of each anchor cable is small; When the strength reduction coefficient is 1.50, each curve turns, and the internal force of the anchor cable suddenly increases, and the anchor cable plays a role. When the strength reduction coefficient is greater than 1.5 and less than 3.27, the internal force of the anchor cable continues to increase. When the strength reduction coefficient is 3.27, the curve turns again, the internal force of the anchor cable continues to increase, and the anchor cable continues to play a role.
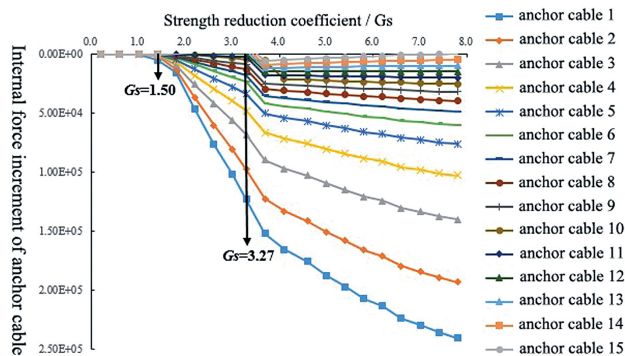

Fig. 4. The relationship between the displacement of the slope and the strength reduction factorwhen the prestress is 500 kN

Figure 4 shows the internal force increment diagram of the anchor cable under different strength reduction factors when the initial prestress of the anchor cable is 500 kN. When the strength reduction coefficient is less than 1.50, with the increase of the strength reduction coefficient, the internal force increment of each anchor cable is small; when the strength reduction coefficient is 1.50, each curve turns, and the internal force of the anchor cable suddenly increases, and the anchor cable plays a role. When the strength reduction coefficient is greater than 1.5, and less than 3.27, the internal force of the anchor cable continues to increase. When the strength reduction coefficient is 3.27, the curve turns again, the internal force of the anchor cable continues to increase, and the anchor cable continues to play a role.

The relationships between the slope toe displacement u and internal force increment ΔF with strength reduction factor are plotted (Fig. 5). In Fig. 5, both the u versus G_s
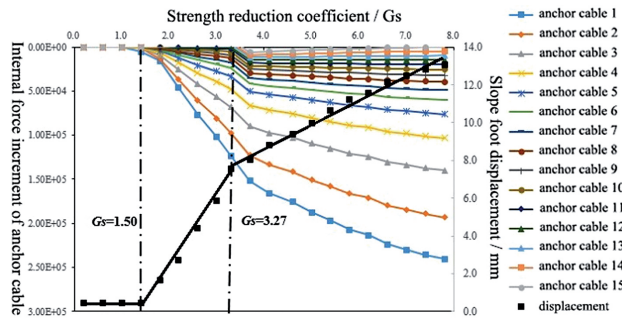
Fig. 5. Curves of internal force the increment and slope displacement of anchor cables and strength reduction coefficient at 500 kN

curve and the ΔF versus G_s curve turn at strength reduction coefficients of 1.50 and 3.27, with good correspondence. This finding shows that the safety factor of the slope can be determined by varying the anchor cable internal force, and the state of the slope stability can be judged.

3. Discussion of the relationship between internal force change in anchor cables and strength reduction coefficient

To study the relationship between the change in internal force of anchor cables and the strength reduction coefficient under different prestresses, the slope model of different prestress reinforcements is established, and the internal force increment of anchor cables under different strength reduction coefficients of the slope is calculated. Figs. 6a–f show the relationship between the internal force increment ΔF and the strength reduction factor G_s of different anchor cables under initial prestresses of 300, 400, 500, 600, 700, and 800 kN, respectively.

There are two obvious turning points (λ_1 and λ_2 in Fig. 6). When the strength reduction coefficient $G_s < \lambda_1$, with the increase of G_s, the curve develops steadily, and each anchor cable begins to play a role, but internal force increases slightly; when the strength reduction coefficient reaches λ_1, the curve suddenly turns and the internal force of the anchor cable increases. When $\lambda_1 < G_s < \lambda_2$, with the increase of G_s, the internal force of anchor cables 1 to 5 near the slope toe increases, while the internal force in anchor cables 6 to 15 far from the slope toe increases slightly. When the strength reduction coefficient is λ_2, the curve turns again, the rate of change reaches the maximum, and the internal force in each anchor cable increases fastest. When the strength reduction coefficient $G_s > \lambda_2$, the internal force of anchor cables 1 to 5 increases more significantly, and anchor cables 6 to 15 also begin to play a role. In increasing the strength reduction coefficient, the internal force increment of anchor cable 1 near the slope toe is the largest, and the increase is the most obvious.
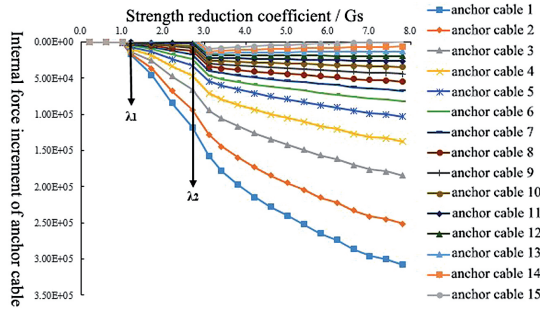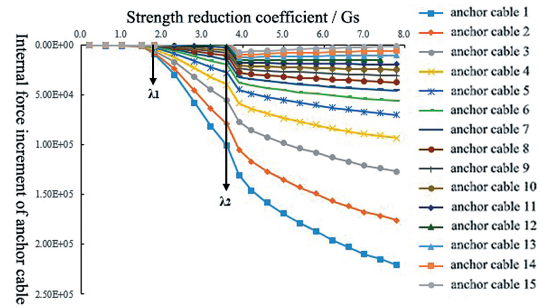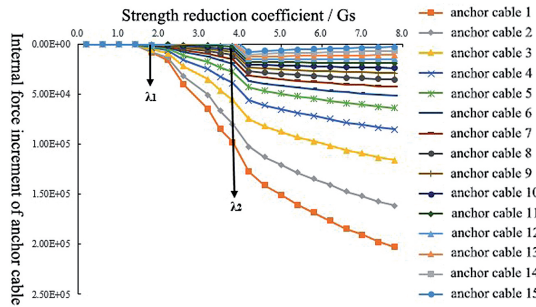
(a) Initial prestress 300 kN
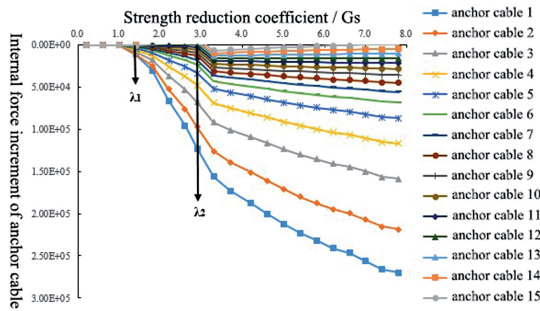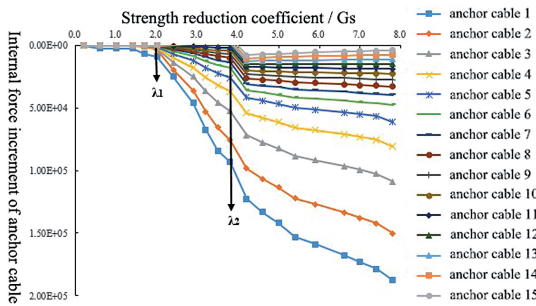

(b) Initial prestress 400 kN
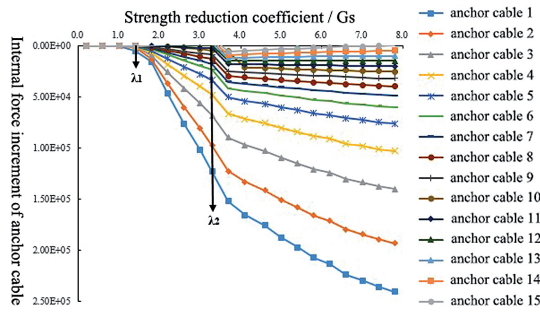
(c) Initial prestress 500 kN

(d) Initial prestress 600 kN

(e) Initial prestress 700 kN

(f) Initial prestress 800 kN

Fig. 6. Internal force increment and strength reduction coefficient of different anchor cables

The λ_1 and λ_2 values and safety factors of the anchor cable slope under the conditions of 300, 350, 400, 450, 500, 550, 600, 650, 700, 750, and 800 kN initial prestress are listed in Table 1. Meanwhile, the relationship between initial prestresses and safety factors (λ_1, and λ_2) is depicted in Fig. 7. With the increase of prestress, the safety factors (λ_1, and λ_2) gradually increase and tend to be stable, and the trends in the increase of the safety factors (λ_1, and λ_2) are consistent.
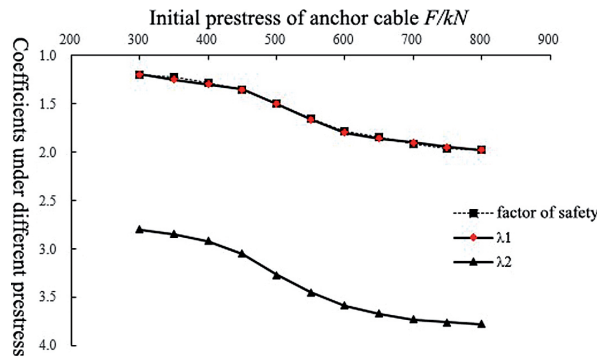

Fig. 7. The relationship between the anchor cable prestress and the safety factors (λ_1, and λ_2)

Table 1. λ_1, λ_2 values of different prestressed anchor cables

Prestress/ kN	300	350	400	450	500	550	600	650	700	750	800
Safety factor	1.20	1.23	1.28	1.36	1.50	1.65	1.78	1.87	1.93	1.96	1.98
λ_1	1.20	1.25	1.31	1.35	1.50	1.66	1.80	1.86	1.90	1.95	1.98
λ_2	2.80	2.85	2.92	3.05	3.27	3.45	3.59	3.67	3.73	3.76	3.78

4. Slope warning method based on the internal force increment ratio of anchor cables

4.1. Slope classification warning

Wu [7] proposed the use of the slope safety factor as the warning index in the landslide state warning criterion. Table 2 lists the values of the internal force increment of anchor cables when the strength reduction coefficient of slope rock mass corresponds to the safety factor under different prestresses. Table 2 demonstrates that when the slope toe begins to slide, the internal force increment of the anchor cable is insignificant, and the internal force of the upper anchor cable has no noticeable change, indicating that the reinforcement effect of the anchor cable on the slope has not been fully exerted. This state only implies that the slope begins to enter the unstable state, which should be used as the starting point for the early warning.

Table 2. The internal force increment value of the cable when the strength reduction factor is equal to the safety factor

Prestress/ kN	300	350	400	450	500	550
Internal force increment/ kN	22.7	21.1	20.8	20.5	19.4	17.5
Prestressed/ kN	600	650	700	750	800	
Internal force increment/ kN	16.8	16.2	12.5	11.5	10.1	

According to the analysis of Section 3, as the strength reduction coefficient exceeds the safety factor λ_1, the displacement of the slope toe increases rapidly, the internal force of the anchor cable increases, and the sliding zone of the slope develops upwards. The unstable state of the slope further develops. When the strength reduction coefficient is equal to λ_2, the rate of increase in the internal force of the anchor cable reaches the maximum, and the internal force increases significantly. At this time, the sliding zone of the slope runs through, the slope enters the dangerous state from the unstable state, and the risk increases.

Therefore, based on the above analysis, the internal force increment of the anchor cable corresponding to λ_1 and λ_2 can be used as two different warning levels, that is, the internal force increment of the anchor cable with the strength reduction coefficient of λ_1 is used as the first warning point, and the increase in the internal force of the anchor cable with

the strength reduction coefficient of λ_2 is used as the second warning point, to realize the classification warning management of the anchor slope.

4.2. The internal force increment of anchor cable

It can be seen from Table 2 that the increment of internal force corresponding to the safety factor of a slope under different prestresses is different due to the different reinforcement effects of different prestress on the slope. With the increase of prestress, the larger the reinforcement force to overcome the slope sliding. Therefore, the internal force increment of the anchor cable decreases. An early warning index for engineering application is established to eliminate the influence of initial prestress, and the internal force increment ratio k is defined thus:

$$(4.1) \qquad\qquad k = \frac{\Delta F}{F}$$

in the formula, ΔF denotes the internal force increment of the anchor cable, and the unit is N; F is the initial prestress of the anchor cable, and the unit is N.

According to the conclusion drawn from Fig. 6, the closer the anchor cable is to the slope foot, the higher the sensitivity to internal force change; because the internal force increment of anchor cable 1 is the largest, the slope stability can be judged according to the change of the internal force increment ratio of anchor cable 1. Fig. 8 demonstrates the relationship curve between the internal force increment ratio k and the strength reduction factor G_s under different initial prestresses on anchor cable 1. With the increase of initial prestress, the internal force increment ratio of anchor cable under the same strength reduction coefficient decreases continuously, and the variation range of the curve is also diminished. The k versus G_s curves under different prestresses have similar characteristics. The curve is flat when $G_s < \lambda_1$, with the increase of G_s, the k value increases slowly. When $\lambda_1 < G_s < \lambda_2$, k increases with the increase in G_s; when $G_s > \lambda_2$, the slope of the curve suddenly increases, and k changes rapidly.
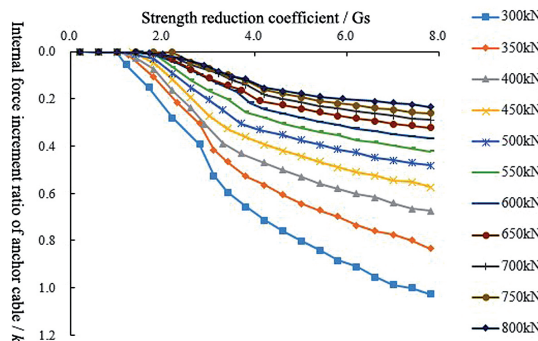

Fig. 8. Curve of internal force increment ratio and strength reduction coefficient of anchor cable

According to the conclusion in Section 4.1, point λ_1 corresponding to the strength reduction coefficient G_s, is the first-level warning point of the slope reinforced by anchor

cables, and point λ_2 is the second-level warning point of the slope reinforced by anchor cables. The λ_1 and λ_2 values under different prestress are corresponding to Fig. 8, and the internal force increment ratios k_1 and k_2 at the warning point are obtained. The k_1 and k_2 values at the early warning point can be used as early warning indexes for evaluating slope stability (Table 3).

Table 3. k_1 and k_2 values of different prestressed anchor cables

Prestress/ kN	300	350	400	450	500	550
k_1	0.076	0.061	0.052	0.046	0.039	0.032
k_2	0.393	0.362	0.308	0.271	0.247	0.202
Prestressed/ kN	600	650	700	750	800	
k_1	0.028	0.025	0.018	0.016	0.013	
k_2	0.168	0.162	0.140	0.122	0.116	

Figure 9 shows the relationship between the primary warning index value k_1 and the initial prestress under different conditions. With the increase of prestress, the internal force increment ratio decreases. The curve shows an exponential relationship. After fitting, the function can be expressed as:

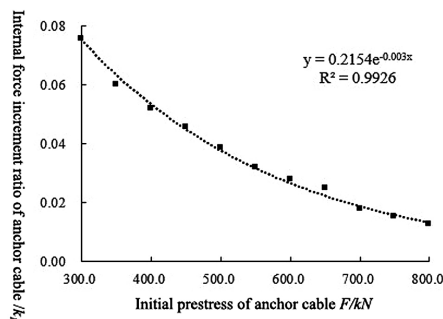$$(4.2) \qquad k_1 = 0.2154e^{-0.003F}$$

Fig. 9. The relationship between the first-level early warning indicator k_1 and the initial prestress

Figure 10 illustrates the relationship between the secondary warning index value k_2 and the initial prestress under different prestresses. With the increase of prestress, the internal force increment ratio decreases gradually. The curve also exhibits an exponential relationship. After fitting, the function can be expressed as:

$$(4.3) \qquad k_2 = 0.8626e^{-0.003F}$$

Based on the relationships as shown in Figs. 9 an 10, the slope early warning threshold and anchor cable prestress show a similar e-index relationship. Therefore, the calculation
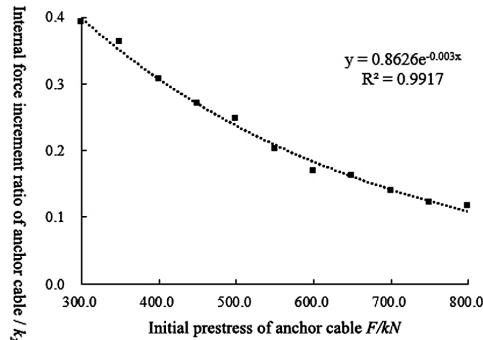
Fig. 10. The relationship between the first-level early warning indicator k_2 and the initial prestress

model of the ratio of initial prestress to the internal force increment of the anchor cable slope is established:

$$(4.4) \qquad\qquad y = Ae^{Bx}$$

where, y is the internal force increment ratio of anchor cables in the slope early warning discriminant index; x represents the initial prestress on an anchor cable; A and B are constants related to the geological conditions of the slope and the nature of the cable itself.

The internal force increment ratio of anchor cables is used as the early warning index of slope stability evaluation, which enriches the slope stability evaluation system. Meanwhile, the multi-index warning method makes the slope warning more accurate.

5. Verification using an engineering project

5.1. Engineering overview

Zhijing River Bridge on the Shanghai-Chongqing Expressway is in the first group, Zhijinghe Village, Badong County (Enshi Tujia and Miao Autonomous Prefecture, Hubei Province, China). The area features complex geological conditions and harsh climate. The stability of the slope where the bridge abutment is built plays a decisive role in the safe operation of the expressway bridge, and it is a key issue in the safe operation of the expressway.

Zhijing River Bridge was constructed on peak clusters and trough valleys formed due to erosion and dissolution, and joint fissures are extremely developed in the mountains on both sides. The surface rocks are seriously weathered, and the surface strata of mountains are somewhat between a weathered residual soil and a fully-weathered rock mass. To ensure stability of the slopes around the Zhijing River Bridge, the support structure combining anchor cables, wire mesh, and shotcrete was applied to the high, steep slopes on both sides of the bridge. The spacing, length, and anchorage length of the anchor cables were separately 3.0 m, 25 to 30 m, and 10 m, and their initial pre-load was 500 kN. The

sections of the slopes with highly fractured rock and soil were also reinforced through grouting.

To assess the potential risk of the slopes timeously, during live operation of the bridge, a section with poor geological conditions was selected as the main monitoring section according to geological data pertaining to the slope. Changes of the long-term pre-load on the anchor cables at the toe of the slope were monitored. The stability of the slope was also assessed in real-time according to the results.

5.2. Judgement of slope stability

Figure 11 shows monitored pre-load data pertaining to key anchor cables in the slope, in which ZXMS-1, ZXMS-2, and ZXMS-3 are separately located near the toe of the slope at the bridge abutment. The monitoring started on July 1, 2019 and lasted for more than two years.
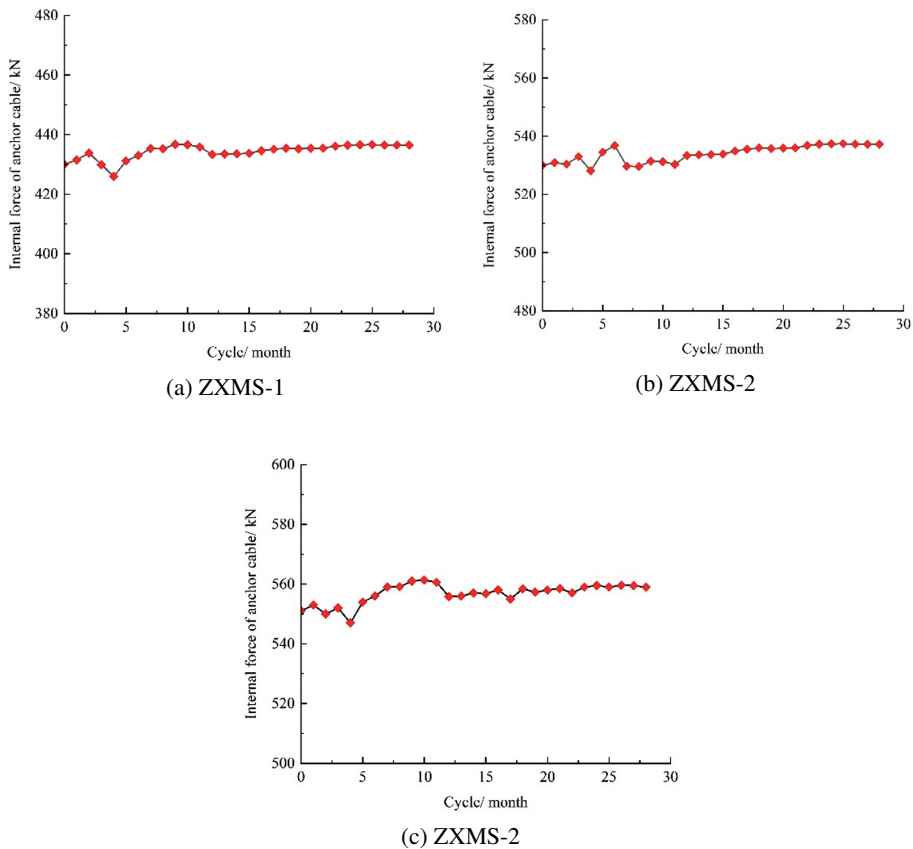

(a) ZXMS-1

(b) ZXMS-2

(c) ZXMS-2

Fig. 11. Monitored internal force of anchor cable

The monitored anchor cable pre-load data show fluctuations under the various environmental influences. For the sake of safety, the maximum change in the anchor cable pre-load was used as the basis for assessing the stability of the slope; according to the results, the specific indices are listed in Table 4.

Table 4 lists the indices summarized according to the research results; the initial pre-loads on three key anchor cables were 430, 530, and 550 kN (values of December 2021), and the maximum increment was between 5 and 8 kN. In accordance with the results, k-values of various anchor cables were between 0.009 and 0.015 (all smaller than the corresponding primary warning index value k_1); the slope was thus deemed stable.

Table 4. k_1 and k_2 values of the monitored anchor cable

Numbering	F/ kN	ΔF/ kN	K	k_1	k_2
ZXMS-1	430	6	0.014	0.059	0.227
ZXMS-2	530	5	0.009	0.044	0.169
ZXMS-3	550	8	0.015	0.041	0.157

5.3. Application suggestions

The method, and indices, used to assess the safety of the slope in the most dangerous sliding state were studied using the theory governing circular slips. It is worth noting that circular sliding is the most common mode of failure in soil slopes, so the results are not completely applicable to rock slopes with relatively intact structures. The results could be applied to severely weathered residual soil slopes with developed joint fissures or soil slopes. The applicability of the present results to rock slopes remains to be further verified.

6. Conclusions

The variations in the displacement of the slope toe and internal force increment of anchor cable with a strength reduction factor of the slope reinforced by different prestressed anchor cables are determined by establishing the calculation model of the high and steep slope. Based on the understanding of the variations of the internal force in an anchor cable, the early warning method and criterion of slope stability are proposed by taking the internal force increment ratio of anchor cables as the early warning index. The following conclusions are obtained as follows:

1. The internal force of anchor cables can be used to judge the stability of slope reinforced by prestressed anchor cables, which is in line with the displacement method and is suitable as the judgment basis for slope monitoring and early warning. The internal force change sensitivity of the anchor cables at the foot of the slope is higher, and the slope stability can be judged by monitoring the internal force change of anchor cables at the foot of a slope;

2. The increment ratio of the anchor cable internal force is established as the early warning index of slope safety and stability. According to the incremental variations of slope anchor cable internal force under different strength reduction coefficients and the corresponding slope stability state, two early warning standards of slope stability state are proposed. When the internal force increment ratio k of anchor cables reaches the first warning standard, the slope begins to enter an unstable state. When k reaches the second warning standard, it shows that the slope sliding zone runs through, and the slope begins to slide;

3. The internal force increment ratio k eliminates the influence of initial prestress, which is convenient for engineering applications. The research implies that the internal force increment ratio of cables in two early warning states shows an e-exponential relationship with prestress, expressed by the formula $y = Ae^{Bx}$. In practical application, the early warning of slope instability with different prestressed reinforcements can be realized through this relationship.

4. The applicability of the method to fully weathered rock and soil slopes was verified based on an engineering project; however, because the method was developed using the theory of circular sliding, it is mainly applicable to soil slopes. Its applicability to rock slopes and the quantitative research on evaluation indices should be further studied based on specific cases and in combination with various other mode of slope failure.

References

[1] J. Li, S.X. Chen, and F. Yu, "Discussion on reinforcing high and steep slope mechanism with prestressed anchor cable", *Rock and Soil Mechanics*, vol. 41, no. 2, pp. 707–713, 2020, DOI: 10.16285/j.rsm.2019.0034.

[2] D.F. Li, Y.L. Zhang, and C.X. Chen, "Design of prestressed-cable sommer for slope-reinforcing engineering", *Rock and Soil Mechanics*, vol. 21, no. 2, pp. 170–172, 2000, DOI: 10.16285/j.rsm.2000.02.019.

[3] S.G. Du, "Method of equal accuracy assessment for the stability analysis of large open-pit mine slopes", *Chinese Journal of Rock Mechanics and Engineering*, vol. 37, no. 6, pp. 1301–1331, 2018, DOI: 10.13722/j.cnki.jrme.2018.0158.

[4] V. Kamchoom and A.K. Leung, "Hydro-mechanical reinforcements of live poles to slope stability", *Soils and Foundations*, vol. 58, no. 6, pp. 1423–1434, 2018, DOI: 10.1016/j.sandf.2018.08.003.

[5] Y.A. Kim, H.I. Lee, K. wan Ko, and T.H. Kwon, "Centrifuge modeling and analytical validation of seismic amplification in a slope during earthquakes – Implications to seismic slope stability analysis", *Soil Dynamics and Earthquake Engineering*, vol. 163, art. no.107502, 2022, DOI: 10.1016/j.soildyn.2022.107502.

[6] B. Li, "Study on Safety Evaluation Index of Slope Prestressed Anchor Cable". [Online]. Available: https://kns.cnki.net/kcms/detail/detail.aspx?dbcode=CMFD{&}dbname=CMFD201301{&}filename= 1012048737.nh{&}uniplatform=NZKPT{&}v=gMBXNtI3p1osOk2JFD7ozGcRDT7v_lNBgWPuY9Gp_ _NO9_FAxE8MjcxgYFKC3fRn.

[7] C. Millot, C. Quantin-Nataf, C. Leyrat, V. Lherm, and M. Volat, "Assessing slope uncertainties of martian Digital Elevation Models from numerical propagation of errors on synthetic geological surfaces", *Icarus*, vol. 391, art. no. 115341, 2022, DOI: 10.1016/j.icarus.2022.115341.

[8] J. Zaczek-Peplinska and M. Kowalska, "Application of non-contact geodetic measurement techniques in dam monitoring", *Archives of Civil Engineering*, vol. 66, no. 3, pp. 49–70, 2022, DOI: 10.24425/ace. 2022.141873.

[9] S.Y. Zhao, Y.R. Zheng, and Y.F. Zhang, "Study on slope failure criterion in strength reduction finite element method", *Rock and Soil Mechanics*, vol. 26, no. 2, pp. 332-336, 2005, DOI: 10.16285/j.rsm.2005.02.035.

[10] D.D. Env, *Eurocode 7: Geotechnical design*. UK, 1997.

[11] J.C. Gu, J. Shen, A.M. Chen, and Z.Q. Ming, "Model Testing Study of Strain Distribution Regular in Rock Mass Caused by Prestressed Anchorage Cable", *Chinese Journal of Rock Mechanics and Engineering*, no. S1, pp. 917–921, 2000. [Online]. Available: https://kns.cnki.net/kcms/detail/detail.aspx.

[12] D.V. Griffiths and R.M. Marquez, "Three-dimensional slope stability analysis by elasto-plastic finite elements", *Geotechnique*, vol. 57, no. 6, pp. 537–546, 2007, DOI: 10.1680/geot.2007.57.6.537.

[13] Z.Q. Liu, C.Y. Zhou, L.G. Dong, X.R. Tan, and Y.M. Deng, "Slope stability and strengthening analysis by strength reduction FEM", *Rock and Soil Mechanics*, vol. 26, no. 4, pp. 558–561, 2005, DOI: 10.16285/j.rsm.2005.04.010.

[14] F.M. Zhang, W.B. Zhao, N. Liu, and Z.Y. Chen, "Long-Term Performance and Load Predtion Model Of Prestressed Cables", *Chinese Journal of Rock Mechanics and Engineering*, vol. 23, no. 1, pp. 39–43, 2004, DOI: 10.3321/j.issn:1000-6915.2004.01.008.

[15] X.L. Ding, Q. Sheng, J. Han, L.K. Cheng, and S.W. Bai, "Nerical Simulation Testing Study on Reinforcement Mechanism of Prestressed Anchorage Cable", *Chinese Journal of Rock Mechanics and Engineering*, vol. 21, no. 7, pp. 980–988, 2002, DOI: 10.3321/j.issn:1000-6915.2002.07.009.

[16] Y. Zhu, T. Ishikawa, S.S. Subramanian, and B. Luo, "Early warning system for rainfall- and snowmelt-induced slope failure in seasonally cold regions", *Soils and Foundations*, vol. 61, no. 1, pp. 198–217, 2020, DOI: 10.1016/j.sandf.2020.11.009.

[17] J. Eichenberger, A. Ferrari, and L. Laloui, "Early warning thresholds for partially saturated slopes in volcanic ashes", *Computers and Geotechnics*, vol. 49, no. 1, pp. 79–89, 2013, DOI: 10.1016/j.compgeo.2012.11.002.

[18] S.S. Subramanian, T. Ishikawa, and T. Tokoro, "An early warning criterion for the prediction of snowmelt-induced soil slope failures in seasonally cold regions", *Soils and Foundations*, vol. 58, no. 3, pp. 582–601, 2018, DOI: 10.1016/j.sandf.2018.02.021.

[19] M. Chen and Q. Jiang, "An early warning system integrating time-of-failure analysis and alert procedure for slope failures", *Soils and Foundations*, vol. 272, art. no. 105629, 2020, DOI: 10.1016/j.enggeo.2020.105629.

[20] H. Zhu, Q. Xiang, B. Luo, Y. Du, and M. Li, "Evaluation of failure risk for prestressed anchor cables based on the AHP-ideal point method: An engineering application", *Engineering Failure Analysis*, vol. 138, art. no. 106293, 2022, DOI: 10.1016/j.engfailanal.2022.106293.

[21] A.P. Dyson and A. Tolooiyan, "Comparative Approaches to Probabilistic Finite Element Methods for Slope Stability Analysis", *Simulation Modelling Practice and Theory*, vol. 100, art. no. 102061, 2020, DOI: 10.1016/j.simpat.2019.102061.

[22] S. Alemdag, A. Kaya, M. Karadag, et al., "Utilization of the limit equilibrium and finite element methods for the stability analysis of the slope debris: An example of the Kalebasi District (NE Turkey)", *Journal of African Earth Sciences*, vol. 106, pp. 134–146, 2015, DOI: 10.1016/j.jafrearsci.2015.03.010.

[23] H. Michalak and P. Przybysz, "Subsoil movements forecasting using 3D numerical modeling", *Archives of Civil Engineering*, vol. 67, no. 1, pp. 367–385, 2021, DOI: 10.24425/ace.2021.136478.

[24] X. Zhang, S. W. Zhou, Y.S. Li, J.H. Pan, and S. Jiang, "Early Warning Criterion and Parameter Sensitivity Analysis of Argillaceous Sandstone Slope", *Journal of Yangtze River Scientific Research Institute*, vol. 36, no. 3, pp. 90–97, 2019, DOI: 10.11988/ckyyb.20170963.

[25] C. Li, J.B. Zhu, B. Wang, Y.Z. Jiang, X.H. Liu, and P. Zheng, "Critical deformation velocity of landslides in different deformation phases", *Chinese Journal of Rock Mechanics and Engineering*, vol. 35, no. 7, pp. 1407–1414, 2016, DOI: 10.13722/j.cnki.jrme.2015.1548.

[26] S.R. Wu, Y.M. Jin, J.S. Shi, Y.S. Zhang, J.L. Han, H. Feng, and D. Chen, "A primary study on landslide warning criterion—An example from the reservoir region of the Three Gorges", *Journal of Jilin University*, vol. 34, no. 4, pp. 596–600, 2004, DOI: 10.13278/j.cnki.jjuese.2004.04.020.

[27] C. Wang, S.R. Zhang, F.H. Zhang, and C.B. Du, "A dynamic simulation analysis method of high-steep slopes based on real-time numerical model and its applications", *Rock and Soil Mechanics*, vol. 37, no. 8, pp. 2383–2390, 2016, DOI: 10.16285/j.rsm.2016.08.034.

[28] Y.P. Wang, Q. Xu, G. Zheng, and H. J, Zheng, "A rheology experimental investigation on early warning model for landslide based on inverse-velocity method", *Rock and Soil Mechanics*, vol. 36, no. 6, pp. 1606–1614, 2015, DOI: 10.16285/j.rsm.2015.06.011.

[29] M. Yang, N. Li, H.R. Li, and G.F. Li, "Evaluation of stability of toppling slope by increment method of anchoring cable stress", *Hydro-Science and Engineering*, vol. 2, no. 2, pp. 8–15, 2019, DOI: 10.16198/j.cnki.1009-640x.2019.02.002.

[30] Y.F. Wang, Y.H. Wang, and H.Y. X, "Computing of the Anchor by the Method of Three-Dimension Point-Radiate Infinite Elements", *Journal of China University of Geosciences*, vol. 18, no. 2, pp. 185–190, 2007, DOI: 10.1016/S1002-0705(07)60036-3.

[31] Q. Xu, et al., "Successful implementations of a real-time and intelligent early warning system for loess landslides on the Heifangtai terrace, China", *Engineering Geology*, vol. 278, art. no. 105817, 2020, DOI: 10.1016/j.enggeo.2020.105817.

[32] F.A.B. Danziger, B.R. Danziger, and M.P. Pacheco, "The simultaneous use of piles and prestressed anchors in foundation design", *Engineering Geology*, vol. 87, no. 3-4, pp. 163–177, 2006, DOI: 10.1016/j.enggeo.2006.06.003.

[33] M.A. Wadee, N. Hadjipantelis, J.B. Bazzano, L. Gardner, and J.A. Lozano-Galant, "Stability of steel struts with externally anchored prestressed cables", *Journal of Constructional Steel Research*, vol. 164, art. no. 105790, 2020, DOI: 10.1016/j.jcsr.2019.105790.

[34] S. Ye, G. Fang, and Y. Zhu, "Model establishment and response analysis of slope reinforced by frame with prestressed anchors under seismic considering the prestress", *Soil Dynamics and Earthquake Engineering*, vol. 122, pp. 228–234, 2019, DOI: 10.1016/j.soildyn.2019.03.034.

[35] N. Li, S.F. Guo, and X.C Yao, "Further study of stability analysis methods of high rock slopes", *Rock and Soil Mechanics*, vol. 39, no. 2, pp. 397–416, 2018, DOI: 10.16285/j.rsm.2017.1323.

[36] G. Wang, B. Zhao, B. Wu, C. Zhang, and W. Liu, "Intelligent prediction of slope stability based on visual exploratory data analysis of 77 in situ cases", *International Journal of Mining Science and Technology*, in press, 2022, DOI: 10.1016/j.ijmst.2022.07.002.

[37] M. Yan, Y. Xia, T. Liu, and V. M. Bowa, "Limit analysis under seismic conditions of a slope reinforced with prestressed anchor cables", *Computers and Geotechnics*, vol. 108, pp. 226–233, 2019, DOI: 10.1016/j.compgeo.2018.12.027.

[38] H. Michalak and P. Przybysz, "Subsoil movements forecasting using 3D numerical modeling", *Archives of Civil Engineering*, vol. 67, no. 1, pp. 367–385, 2021, DOI: 10.24425/ace.2021.136478.

[39] S. Weglinski, M. Flieger-Szymańska, M. Just and D.A. Krawczyk, "Ground improvement and rebuild of a district road in complex geotechnical-engineering conditions–case study", *Archives of Civil Engineering*, vol. 68, no. 2, pp. 63–82, 2022, DOI: 10.24425/ace.2022.140630.

[40] A. Al-Sabouni-Zawadzki, A. Zawadzki, "Simulation of a Deployable Tensegrity Column Based on the Finite Element Modeling and Multibody Dynamics Simulations", *Archives of Civil Engineering*, 2020, vol. 66, no. 4, pp. 543–560, 2020, DOI: 10.24425/ace.2020.135236.